*Proc. Natl. Acad. Sci. USA*
Vol. 90, pp. 1701–1705, March 1993
Medical Sciences

# Defective proα2(I) collagen synthesis in a recessive mutation in mice: A model of human osteogenesis imperfecta

(*oim* gene/homotrimeric collagen/skeletal deformity/murine *Cola-2* gene)

STEWART D. CHIPMAN*†, HOPE O. SWEET‡, DANIEL J. MCBRIDE, JR.*, MURIEL T. DAVISSON‡, SANDY C. MARKS, JR.§, ALAN R. SHULDINER*, RICHARD J. WENSTRUP¶, DAVID W. ROWE‖, AND JAY R. SHAPIRO*,**

*Bone Metabolism Research Laboratory, Division of Geriatric Medicine and Gerontology, Johns Hopkins University School of Medicine, Baltimore, MD 21224; ‡Mutant Mouse Resource, The Jackson Laboratory, Bar Harbor, ME 04609; §Department of Cell Biology, University of Massachusetts Medical School, Worcester, MA 01655; ¶Department of Dermatology, Duke University Medical Center, Durham, NC 27710; and ‖Department of Pediatrics, University of Connecticut Health Science Center, Farmington, CT 06032

*Communicated by Darwin J. Prockop, June 23, 1992 (received for review December 10, 1991)*

**ABSTRACT** **Osteogenesis imperfecta (OI) is a heritable disorder of connective tissue associated with fractures, osteopenia, and short stature. OI results from mutations affecting the proα1 or proα2 gene of type I collagen. We describe a strain of mice with a nonlethal recessively inherited mutation (*oim*) that results in phenotypic and biochemical features that simulate moderate to severe human OI. The phenotype of homozygous *oim* mice includes skeletal fractures, limb deformities, generalized osteopenia, and small body size. Their femurs are smaller and demonstrate marked cortical thinning and fewer medullary trabeculae than those of wild-type mice. Breeding studies show the mutation is inherited in most crosses as a single recessive gene on chromosome 6, near the murine *Cola-2* gene. Biochemical analysis of skin and bone, as well as isolated dermal fibroblast cultures, demonstrate that α1(I) homotrimeric collagen accumulates in these tissues and is secreted by fibroblasts. Short labeling studies in fibroblasts demonstrate an absence of proα2(I) collagen chains. Nucleotide sequencing of the cDNA encoding the COOH-propeptide reveals a G deletion at proα2(I) nucleotide 3983; this results in an alteration of the sequence of the last 48 amino acids. The *oim* mouse will facilitate the study of type I collagen-related skeletal disease.**

Osteogenesis imperfecta (OI) is a heritable disorder of connective tissue whose primary clinical features in humans include multiple fractures, skeletal deformities, osteopenia, short stature, blue sclerae, and joint laxity. The application of techniques in protein biochemistry and molecular biology during the past decade has indicated that the majority of OI patients have mutations of the proα1 or proα2 chain of type I collagen (1, 2). These studies have utilized isolated dermal fibroblast and/or iliac crest osteoblast cultures (3). A viable animal model of OI based on a type I collagen mutation would facilitate investigation of the role of defective type I collagen on skeletal tissue formation.

Although imperfect osteogenesis has been previously observed in bovine, feline, and murine species, none of these have duplicated both the biochemical and clinical findings associated with human OI (4–7). The *Mov-13* mouse, which has a transcriptional block of the proα1(I) collagen gene, has provided a potential model of human OI type II (8–13). More recently, several transgenic variants of *Mov-13* and normal mice have been created as useful models of mild OI type I or lethal OI type II (††, 14, 15).

In this report we describe a naturally occurring mouse mutation that produces phenotypic and biochemical features similar to those seen in moderate to severe human OI. We have named this mutation osteogenesis imperfecta murine (*oim*). Homozygous *oim* mice have osteopenia, fractures, and progressive skeletal deformities. Our data indicate that these mice are deficient in proα2(I) collagen because of a G deletion at nucleotide 3983 of the *Cola-2* gene. This mutation results in tissue accumulation of α1(I) homotrimeric collagen in the extracellular matrix. Homozygous *oim* mice should permit the study of type I collagen pathophysiology in a manner not possible in humans.

## MATERIALS AND METHODS

**Radiographic and Microscopic Examination.** Whole-body radiographs were taken in a Faxitron x-ray machine (34 keV for 1.5 min) using Kodak OM1 film. For light microscopy, excised femurs were fixed in neutral buffered Formalin for 24 hr, decalcified in 10% (wt/vol) EDTA in 0.1 M Tris·HCl buffer, pH 6.9, for 14 days at 4°C, embedded in paraffin, sectioned, and stained with hematoxylin and eosin.

**Isolation and Culture of Dermal Fibroblasts.** Dermis was obtained from the back of 3- to 5-day-old homozygous *oim* and wild-type pups. The skin was rinsed with iodine then 70% (vol/vol) ethanol, excised, and minced to 1- to 3-mm$^2$ pieces. Explants were grown for 2 weeks in Dulbecco's modified Eagle's medium supplemented with 10% fetal bovine serum, streptomycin at 100 μg/ml, penicillin at 100 units/ml, and amphotericin B at 0.25 μg/ml. Cultures were assayed in the second passage.

**Collagen and Procollagen Analysis *in Vitro*.** Fibroblast cultures were grown several days past visual confluence in 10-cm$^2$ dishes. The medium was then supplemented with 150 μM sodium ascorbate and 24 hr later the cultures were incubated for 30 min in Dulbecco's modified Eagle's medium plus 1% dialyzed fetal bovine serum, antibiotics, 100 μM each nonessential amino acids but no proline, and 150 μM sodium ascorbate (starve medium). *De novo* synthesized proteins were radiolabeled for 2 hr (short-label analysis) or 24 hr (steady-state analysis) with starve medium containing 20 μCi (1 Ci = 37 GBq) of L-[2,3,4,5-$^3$H]proline in 1 ml of starve medium per 10-cm$^2$ culture dish.

The publication costs of this article were defrayed in part by page charge payment. This article must therefore be hereby marked "*advertisement*" in accordance with 18 U.S.C. §1734 solely to indicate this fact.

Abbreviation: OI, osteogenesis imperfecta.

†Present address: OsteoArthritis Sciences, Inc., Cambridge, MA 02139.

**To whom reprint requests should be addressed at: Bone Metabolism Research Laboratory, Johns Hopkins University Asthma and Allergy Center, 5501 Hopkins Bayview Circle, Baltimore, MD 21224.

††Khillan, J. S., Olsen, A. S., Kontusaari, S. & Prockop, D. J., Third International Conference on the Molecular Biology and Pathology of Matrix, Jefferson Institute of Molecular Medicine, Philadelphia, 1988 (abstr.).

For the 24-hr steady-state analysis, the combined cell layer and medium fractions were harvested in phosphate-buffered saline containing proteolysis inhibitors (5 mM EDTA, 1 mM *p*-hydroxymercuribenzoate, 5 mM *N*-ethylmaleimide, and 100 $\mu$M phenylmethylsulfonyl fluoride). The sample was then homogenized with a Broeck tissue grinder and precipitated with 30% (vol/vol) ethanol at 4°C. Limited pepsin digestion was performed with 100 $\mu$g of pepsin per tube for 2 hr at 4°C. The resistant $\alpha$-chains were precipitated with 4.5 M NaCl/50 mM Tris·HCl, pH 7.5, and centrifuged at 10,000 × *g*, and the pellet was washed with 18% (vol/vol) ethanol. An aliquot of this material was utilized to determine the thermal stability of the type I collagen triple helix (16). An aliquot was reconstituted in sample buffer and, following heat denaturation, the $\alpha$-chains were separated by SDS/7.5% PAGE under delayed reduction conditions (17). The gel was prepared for autoradiography (En$^3$Hance; NEN), dried, and exposed for 48 hr to Kodak XAR-5 film at −70°C. Collagen $\alpha$-chain migration and $\alpha 1/\alpha 2$ ratios were assessed by scanning densitometry.

For the 2-hr short-label analysis, the cell layer alone was harvested in phosphate-buffered saline containing proteolysis inhibitors. The sample was then homogenized with a Broeck tissue grinder and precipitated with 30% ethanol at 4°C. The pro$\alpha$-chains were washed with 4.5 M NaCl/50 mM Tris·HCl, pH 7.5, and centrifuged at 10,000 × *g*, and the pellet was washed with 18% ethanol and then analyzed by SDS/PAGE without reduction.

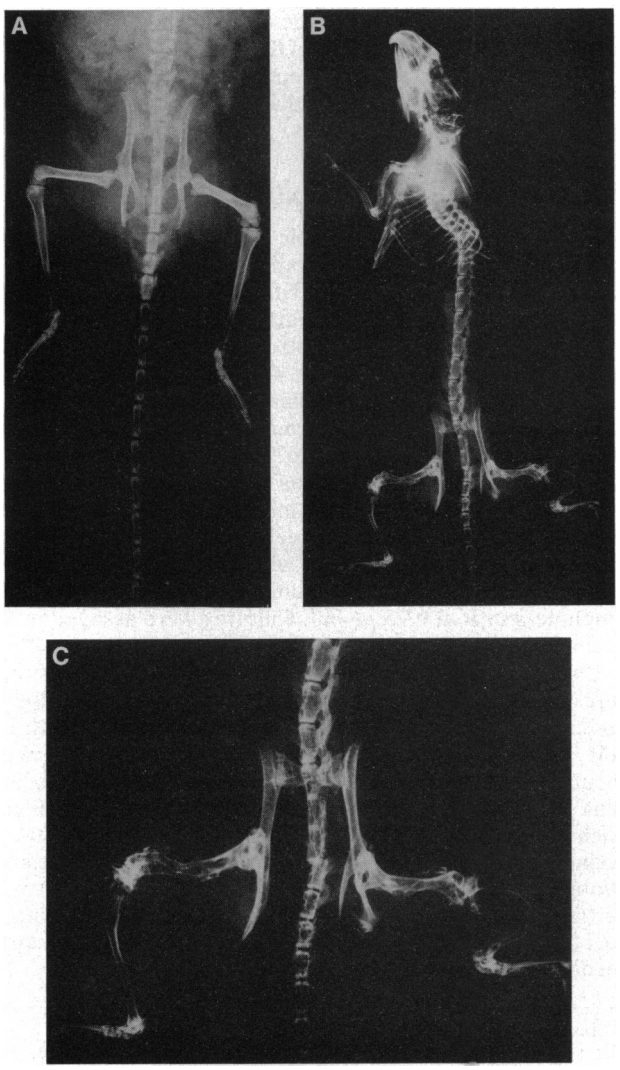


FIG. 1. (*A*) Radiograph of normal bone structure in a 7-month-old wild-type mouse. (×1.1.) (*B*) Radiograph of a 13-month-old homozygous *oim* mouse showing generalized osteopenia, marked cortical thinning, bowing of the long bones, scoliosis, sclerosis around the knee joints, and a pronounced dorsal kyphosis. (×0.9.) (*C*) Pelvic radiograph of the homozygous *oim* mouse in *B*, showing bowing of the long bones, sclerosis around the knee joints, and fracture callus. (×2.0.)

**Type I Collagen Nucleotide Sequencing.** Total RNA was isolated either from the tails of homozygous *oim* mice or from dermal fibroblast cultures isolated from wild-type mice by using RNAzol (Cinna/Biotex, Friendswood, TX). Reverse transcriptase/polymerase chain reaction (RT-PCR) was used to generate cDNA fragments from the COOH-propeptide region of the pro$\alpha$2(I) mRNA. Total RNA was reverse transcribed by using the RACE 1 oligonucleotide [5′-GAT GGA TCC TGC AGA AGC $(T)_{17}$-3′], reverse transcriptase, and a mixture of dNTPs (18). An aliquot of the first-strand synthesis reaction, the downstream oligonucleotide RACE 2 (5′-GAT GGA TCC TGC AGA AGC-3′) and an upstream coding oligonucleotide (5′-TCC AAG GAA ATG GCA ACT CAG CTC-3′) were used for second-strand synthesis and PCR amplification (19). A total of 35 cycles were performed in a thermal cycler, consisting of initial denaturation at 94°C for 5 min, followed by 34 cycles of annealing at 50°C for 1 min, extension at 72°C for 1 min, denaturation at 94°C for 1 min, and then a final annealing at 50°C for 1 min and extension at 72°C for 10 min. PCR products were analyzed by 1% agarose gel electrophoresis and ethidium bromide staining. cDNAs of the expected size were electroeluted from preparative gel slices and an aliquot was used for direct nucleotide sequencing by the Sanger method, using an ABI model 373A automated DNA sequencer (Applied Biosystems). A second aliquot of the purified PCR product was cloned in a TA 1000 cloning plasmid (Invitrogen). The plasmid was purified with a Qiagen (Studio City, CA) Maxi Prep Kit prior to sequencing the insert.

## RESULTS

A mouse with severe skeletal deformity occurred in the Mutant Mouse Resource of The Jackson Laboratory. The *oim* (osteogenesis imperfecta murine) mutation first occurred in an $F_2$ intercross between C3H/HeJ and C57BL/6JLe mice. Currently, the *oim* mutation is maintained on the B6C3Fe-*a*/*a* (C57BL/6JLe × C3HeB/FeJLe-*a*/*a*) hybrid background by the cross-intercross system of mating. Homozygous *oim* mice of both sexes are fertile. More than 50 homozygous *oim* mice have been bred to date. Homozygous *oim* mice live approximately 1.25 ± 0.25 years; premature mortality has not been noted.

Homozygous *oim* mice can often be identified at birth by the appearance of hemorrhages into joint cavities, sides of the body, or around the scapulas; visible breaks in the long bones of the legs; a "drooping wrist" appearance due to subluxation on one or both forepaws; and periodically noticeable breaks in the tail vertebrae. Radiographs of the pelvis of a 7-month-old (middle-aged) homozygous *oim* mouse, compared with a wild-type mouse, demonstrated several features typical of OI, including evidence of healed fractures, long bone deformities, generalized osteopenia, and marked cortical thinning (Fig. 1 *A*). The progressively deforming nature of the *oim* mutation on the skeleton is demonstrated in the radiograph of a 13-month-old (elderly) homozygous *oim*

Table 1. Body weights of 6- to 9-month-old homozygous *oim* mice and wild-type mice

| Genotype | Sex | *n* | Body weight, g |
|---|---|---|---|
| Wild type | M | 8 | 34.7 ± 2.5 |
| *oim*/*oim* | M | 4 | 25.7 ± 1.8 |
| Wild type | F | 9 | 29.5 ± 1.9 |
| *oim*/*oim* | F | 4 | 23.2 ± 1.0 |

Weights are mean ± SD.

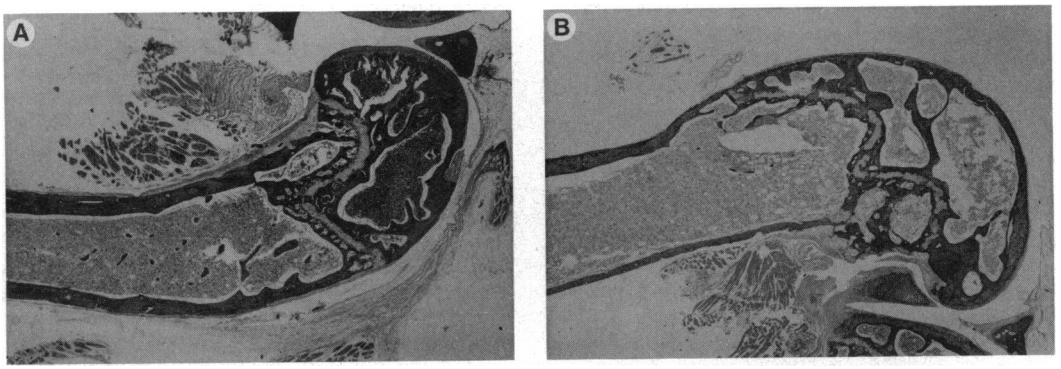


FIG. 2. Representative histological sections of decalcified femurs from 7-month-old wild-type (*A*) and homozygous *oim* (*B*) mice. These demonstrate marked cortical thinning and fewer and thinner trabeculae in the diaphyseal region and femoral head of the homozygous *oim* mouse. (×10.)

mouse (Fig. 1 *B* and *C*). Elderly *oim* mice developed a pronounced dorsal kyphosis (Fig. 1*B*), severely deformed long bones, and an abnormal gait. Homozygous *oim* mice are smaller than age- and sex-matched wild-type mice or unaffected (wild-type or heterozygous *oim*) littermates (Table 1).

Femurs from 7-month-old homozygous *oim* and wild-type mice were examined by light microscopy (Fig. 2). Representative sections of the femur from the homozygous *oim* mouse revealed marked cortical thinning along with fewer medullary trabeculae. Under higher magnification, along with the marked cortical thinning, there appeared to be an increase in the number or density of cortical osteocytes (not shown). There was also a lack of normal lamellar organization of the cortical bone as studied by polarizing microscopy (not shown). Dermal fibroblasts from homozygous *oim* mice had a rounded morphology upon examination by transmission electron microscopy, in contrast to the typical elongated shape seen in an unaffected littermate (wild-type or heterozygous *oim*). In addition, fibroblasts in the skin of homozygous *oim* mice contained greatly dilated cisternae of the rough endoplasmic reticulum (not shown).

In matings of mice carrying the *oim* mutation, the trait usually segregates as a recessive mutation with variable levels of expression (Table 2). However, the genetic background may influence the expression of the external phenotype. An allele test between *oim* and *fro*, a chemically induced mutation that produces a somewhat similar phenotype (3), was negative. Linkage tests with genetic markers on each autosomal chromosome were negative, except that crosses between *oim* and the chromosome 6 marker genes $Mi^{wh}$ (white, a dominant gene causing white spotting) and *wa-1* (a recessive gene causing a curly coat) gave 40% recombination. These markers are located 40 centimorgans from the centromere. Coupling backcross matings with *oim* and $Mi^{wh}$ (*oim* +/+ $Mi^{wh}$ × *oim* +/*oim* +) produced 20 + $Mi^{wh}$, 28 *oim* +, 19 + +, and 13 *oim* $Mi^{wh}$ mice ($n$ = 80 progeny, recombination frequency = 40.00% ± 5.48%). A repulsion intercross between *oim* and *wa-1* (*oim* +/+ *wa-1* × *oim* +/+ *wa-1*) produced 131 + +, 53 *oim* +, 37 + *wa-1*, and 5 *oim wa-1* ($n$ = 226 progeny, recombination frequency = 39.60% ± 4.99%). The recombination percent in the intercross was determined by using a computer program based on Fisher's scores (20).

The finding that the homozygous *oim* mouse was deficient in pro$\alpha$2(I) collagen (see below), along with the knowledge that the murine *Cola-2* structural locus maps to proximal chromosome 6, led us to set up mapping crosses between *oim* and the more proximal markers sightless (*Sig*) and δ-glu-

Table 2. Breeding experiments demonstrating the recessive nature of the *oim* mutation

| Mating | | | No. of progeny with phenotype | | Total no. of progeny | $\chi^2$ |
|---|---|---|---|---|---|---|
| Female | × | Male | Wild type | *oim* | | |
| +/*oim* | × | +/*oim* | 40 | 9 | 49 | 0.1496 |
| +/*oim* | × | +/*oim* | 173 | 59 | 232 | 0.0229 |
| *oim*/*oim* | × | +/*oim* | 42 | 54 | 96 | 1.50 |
| +/*oim* | × | *oim*/*oim* | 23 | 15 | 38 | 1.6842 |
| Combined backcrosses | | | 65 | 69 | 134 | 0.1194 |
| *oim*/*oim* | × | +/+ | 25 | — | 25 | — |
| +/+ | × | *oim*/*oim* | 24 | — | 24 | — |
| *oim*/*oim* | × | *oim*/*oim* | — | 28 | 28 | — |

These data are based on visual classification of the phenotype. The data in line 1 were collected before and the data in line 2 were collected after we began using a phenotypic test to distinguish mutant and normal mice. The phenotypic test was to hold the mouse and gently touch all four paws, then place the mouse on a flat surface. Difficulty in walking was used as an indication that the mice were homozygous *oim*/*oim* mutants. The $\chi^2$ values are for one degree of freedom. These data indicate that there is no significant difference between the observed progeny ratios and those expected for a mating of each type involving a recessive gene (3:1 for lines 1 and 2 and 1:1 for lines 3–5).

Table 3. Linkage analysis of the *oim* position on proximal chromosome 6

Two-point backcross with *Sig*

| Mating | | | No. of progeny with genotype | | | | Total no. of progeny |
|---|---|---|---|---|---|---|---|
| Female | × | Male | *Sig* + | + *oim* | + + | *Sig oim* | |
| $\frac{Sig\ +}{+\ oim}$ | × | $\frac{+\ oim}{+\ oim}$ | 26 | 34 | 1 | 2 | 63 |

Three-point backcross with *Sig* and *Ggc*

| Mating | | | Progeny phenotype | | | | | | No. of progeny (total = 41) |
|---|---|---|---|---|---|---|---|---|---|
| Female | × | Male | *Sig* | | *oim* | | *Ggc* | | |
| | | | *Sig* | × | + | | *ab* | | 12 |
| | | | + | × | *oim* | | *aa* | | 13 |
| $\frac{Sig\ +\ Ggc^b}{+\ oim\ Ggc^a}$ | × | $\frac{+\ oim\ Ggc^a}{+\ oim\ Ggc^a}$ | *Sig* | × | *oim* | | *aa* | | 1 |
| | | | + | × | + | | *ab* | | 1 |
| | | | *Sig* | × | + | × | *aa* | | 5 |
| | | | + | × | *oim* | × | *ab* | | 9 |

For the three-point backcross with *Sig* and *Ggc*, the progeny classes are given as phenotype: *oim* means *oim*/*oim*, + means +/*oim*, *Sig* means *Sig*/+, *ab* means $Ggc^a/Ggc^b$, and *aa* means $Ggc^a/Ggc^a$. Recombination estimate for two-point backcross: 3/63 = 4.76% ± 2.68%. Recombination estimates for three-point backcrosses: *Sig–oim*, 2/41 = 4.88% ± 3.36%; *oim–Ggc*, 14/41 = 34.15% ± 7.41%; and *Sig–Ggc*, 16/41 = 39.02% ± 7.62%.

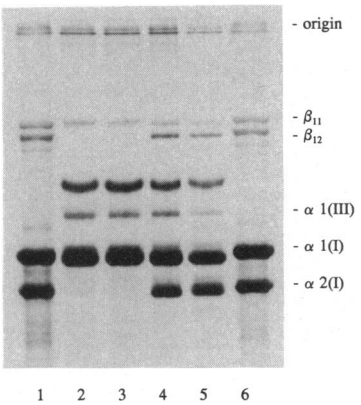


FIG. 3. SDS/7.5% PAGE of type I collagen labeled for 24 hr from homozygous *oim* and wild-type mouse dermal fibroblast cultures. Lanes: 1 and 6, type I collagen standard; 2 and 3, homozygous *oim*; 4 and 5, wild type. Note the absence of the β12 and α2-chain of type I collagen from the homozygous *oim* cells.

tamylcyclotransferase (*Ggc*) (Table 3). Two- and three-point backcrosses with *Sig* and *Ggc*, (C57BL/6J-*Sig* × B6C3H-*oim*)$F_1$ females × B6C3H-*oim*/*oim* males, confirmed linkage of *oim* to proximal chromosome 6 (Table 3). The results of these crosses, assuming the least-frequent class is a double-crossover class, give the following order and distances (centimorgans): centromere–*Sig*–4.8 ± 2.3–*oim*–34.2 ± 7.4–*Ggc*.

Dermal fibroblast cultures were isolated, grown to confluence, and radiolabeled with [$^3$H]proline. Collagens from the combined media and cell layer were separated by SDS/7.5% PAGE after limited pepsin digestion. This analysis demonstrated the absence of α2(I) chains, broadening of the α1(I) band, and normal levels of α1(III) in fibroblasts isolated from two different homozygous *oim* mice (Fig. 3). Densitometric analysis of the autoradiogram demonstrated that the α1/α2 ratio for the wild-type mice was 2.3:1, close to the theoretical 2:1. The homozygous *oim* mice had no detectable α2(I) chains. To further characterize the absence of α2(I) chain synthesis in homozygous *oim* mice we labeled fibroblasts for only 2 hr with [$^3$H]proline. The proα-chains from the cell layer compartment were separated by SDS/7.5% PAGE and visualized by autoradiography. Synthesis of proα2(I) chains was not detected by SDS/PAGE analysis in cultured homozygous *oim* fibroblasts (Fig. 4).

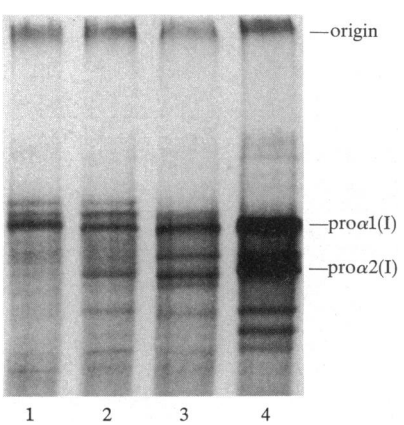


FIG. 4. SDS/7.5% PAGE of type I procollagen isolated from cell layer of homozygous *oim* mouse dermal fibroblast cultures. The cultures had been labeled for 2 hr, for the purpose of examining the short-term accumulation of the proα1 and proα2-chains of type I collagen. Lanes: 1, homozygous *oim*; 2, heterozygous *oim*; 3, wild type; 4, type I procollagen standard.

| aa 1313 | | | | | | | | | | | |
|---|---|---|---|---|---|---|---|---|---|---|---|
| Asp | Gly | Cys | Ser | Lys | Lys | Thr | Asn | Glu | Trp | Gly | wild type |
| GAT | GGC | TGC | TCC | AAA | AAG | ACA | AAT | GAA | TGG | GGC | wild type |
| nt 3964 | | | | | | ▲ nt 3983 | | | | | |
| GAT | GGC | TGC | TCC | AAA | AAA | CAA | ATG | AAT | GGG | GCA | *oim* |
| Asp | Gly | Cys | Ser | Lys | Lys | Gln | Met | Asn | Gly | Ala | *oim* |

FIG. 5. Comparison of wild-type and homozygous *oim* murine nucleotide and amino acid sequences. The wild-type murine *Cola-2* gene has 4098 nucleotides and encodes 1366 amino acids.

On the basis of biochemical similarities with a severely affected OI type III patient initially described by Nichols *et al.* (21, 22) and characterized at the protein and nucleotide level by Prockop and coworkers (23–25), we began the nucleotide analysis of *oim* by sequencing the COOH-terminal propeptide of the *Cola-2* gene. Using the partial murine *Cola-2* nucleotide sequence derived from the murine osteoblast cell line MC3T3-E1, we generated a series of oligonucleotide pairs for reverse transcriptase/PCR (26). Following this approach, we identified a G point deletion at proα2(I) nucleotide 3983 (Fig. 5). This mutation alters the reading frame, resulting in the final 48 amino acids of the COOH-terminal propeptide being incorrect and generating a new translation stop site that causes the addition of an extra amino acid. These data are consistent with the observation of full-length α2(I) mRNA transcripts by Northern analysis (not shown). The G deletion was identified by direct sequencing of PCR products generated from a homozygous *oim* mouse and by sequencing both strands of the PCR product cloned in a plasmid. The deletion was confirmed in a second homozygous *oim* mouse by direct sequencing of the PCR product.

## DISCUSSION

Several phenotypic features of homozygous *oim* mice closely simulate those seen in moderate to severe human OI. Homozygous *oim* mice are born with fractures or develop them at an early age. The generalized radiolucency, cortical thinning, bowing of the long bones, fractures, and calluses as evidence of healed fractures are radiological hallmarks of human OI (1, 27). Other features characteristic of OI included apparent joint subluxation (suggesting laxity), joint hemorrhage (indicating easy bruisability), and dorsal kyphosis (1). Light microscopic examination of a representative section of a homozygous *oim* mouse femur revealed marked cortical thinning and diminished trabecular bone volume. In addition, observation of cortical lamellae by polarized light demonstrated an irregular pattern of birefringence in the mutant mice, suggesting a disorganized collagen matrix. These changes in histological appearance of the long bones have been previously reported in individuals with OI (28).

Recent studies of human OI indicate a prevalence of dominant structural mutations of type I collagen (29). Recessive mutations have been reported to occur in 7% of the severe OI type III patients, where the disease is most often sporadic (30). The *oim* mutation appears to be transmitted as a recessive trait.

The phenotypic, biochemical, and molecular findings in homozygous *oim* mice closely duplicate those seen in the previously mentioned OI type III patient (21–23). We have demonstrated an absence of α2(I) chains in bone and skin and in fibroblast cultures; instead secretion and matrix accumulation of α1(I) homotrimeric collagen was observed. The thermal stability profile of homotrimeric type I collagen isolated from homozygous *oim* fibroblast cultures also duplicates the two-stage thermal melting curve noted for the OI patient (16). Interestingly, in the human case, as well as in the

homozygous *oim* mouse, the expression of α1(I) homotrimeric collagen is consistent with survival.

The α2(I) mutation in the OI patient involved a four-nucleotide deletion in exon 52 in the COOH-terminal portion of the collagen chain (23–25). The G nucleotide deletion in homozygous *oim* mice is located in the same region of the molecule and results in an altered amino acid sequence. A new stop codon is generated that adds one amino acid to the primary sequence.

Several other syndromes affecting connective tissue development and skeletal formation have been reported in mice, including fragilitas ossium (*fro*), grey lethal (*gl*), hypophosphatemia (*Hyp*), microophthalmia (*mi*), osteosclerotic (*oc*), osteopetrosis (*op*), and tight skin (*Tsk*) (31). However, the phenotypes of these mutations are distinctly different from the phenotype observed in the *oim* mouse. The oim mutation is maintained on the B6C3Fe hybrid, which has on average 50% C57BL/6J genetic background. The C57BL/6 strain has been associated with osteopenia and scoliosis in older animals (32). The *oim* mutation, however, segregates as a single autosomal gene, and clinical features are present much earlier in life, distinguishing it from the osteoporosis of old age seen in C57BL/6J.

Syndromes phenotypically simulating OI have been reported to affect cattle (6, 7, 33, 34), cats (5), tigers, and mice (4, 35). No naturally occurring mutation has been demonstrated to adequately replicate both the phenotype and the biochemical lesion observed in human OI. The *Mov-13* mutation in mice was caused by a proviral insertion of the Moloney murine leukemia virus into the first intron of the murine *Cola-1* gene, resulting in a recessive embryonic lethal (OI type II) phenotype (8–11, 36). However, this model does not fully duplicate human OI type II, since the lack of murine *Cola-1* expression results in complete failure to form a skeleton and early *in utero* cessation of development of the vasculature.

Bonadio *et al.* (15) have recently characterized the heterozygous *Mov-13* mice and have proposed the animal as a model for the mild, dominant form of OI (type I). Affected mice have decreased collagen content in the skin, disorganized cortical lamellar structure, diminished bone strength, and reduced hearing associated with half-normal synthesis of type I collagen.

Stacey *et al.* (14) made transgenic mice by the introduction of a murine *Cola-1* genomic clone encoding a substitution of either cysteine or arginine for glycine at position 859. This resulted in a dominant lethal phenotype with skeletal lesions similar to the lethal human OI type II. Transgenic fetuses had a striking reduction in type I collagen production in skin, demonstrating the deleterious effect that a mutant proα1(I) chain can have on production of normal procollagen. This strategy demonstrates the utility of engineered transgenic mice as a type I collagen-based model for OI.

Khillian *et al.* (††) have prepared a minigene version of *Cola-1* extending from −2.5 kb of the promoter region to intron 5. This minigene is joined to a fragment extending from intron 46 to 2 kb beyond the second polyadenylylation site. Progeny of transgenic animals expressing high levels of this transgene died after birth with symmetrically fractured ribs. This mouse may be a model for OI type II.

This report suggests that the homozygous *oim* mouse replicates many of the biochemical and phenotypic findings in moderate to severe human OI. Homozygous *oim* mice as a model of human OI would facilitate investigations of the pathophysiology and structure–function relationships of type I collagen, as well as provide a model to determine the usefulness of medical therapies.

We thank Carole A. MacKay, Shirwin M. Pockwince, Jeaneen Fletcher, Chester R. Frazier, and Kimberly A. Scriven for technical assistance, Kenneth R. Johnson for helpful comments, Ellen C. Akeson for *Ggc* isoenzyme typing, Charlotte L. Phillips for the normal murine DNA sequence, and J.-L. Guénet (Institut Pasteur) for the *fro* allelic test. This work was supported by the following grants from the National Institutes of Health: AR-38370, AR-39737, AR-39870, AR-40926, AR-30426, AR-38933, and CA-34196, by National Science Foundation Grant DIR 8418828, and by gifts from the Eleanor Naylor Dana Charitable Trust, the Jaqua Foundation, the NorthEast Osteogenesis Imperfecta Foundation, the Johns Hopkins University Institutional Research Grant Program, and the Society Bitonto San Cosma y Damiano.

1. Shapiro, J. R. & Chipman, S. D. (1992) in *Collagen: Pathobiochemistry*, eds. Kang, A. & Nimni, M. (CRC, Boca Raton, FL), Vol. 5, pp. 49–86.
2. Byers, P. H., Bonadio, J. F., Cohn, D. H., Starman, B. J., Wenstrup, R. J. & Willing, M. (1988) *Ann. N.Y. Acad. Sci.* **543**, 117–128.
3. Chipman, S. D., Shapiro, J. R., McKinstry, M. B., Stover, M. L., Branson, P. & Rowe, D. W. (1992) *J. Bone Miner. Res.* **7**, 793–808.
4. Guénet, J. L., Stanescu, R., Maroteaux, P. & Stanescu, V. (1981) *J. Hered.* **72**, 440–441.
5. Cohn, L. A. & Meuten, D. J. (1990) *J. Am. Vet. Med. Assoc.* **197**, 98–100.
6. Denholm, L. J. & Cole, W. G. (1983) *Aust. Vet. J.* **60**, 9–17.
7. Termine, J. D., Gehron-Robey, P., Fisher, L. W., Shimokawa, H., Drum, M. A., Conn, K. M., Hawkins, G. R., Cruz, J. B. & Thompson, K. G. (1984) *Proc. Natl. Acad. Sci. USA* **81**, 2213–2217.
8. Schnieke, A., Harbers, K. & Jaenisch, R. (1983) *Nature (London)* **304**, 315–320.
9. Harbers, K., Kuehn, M., Delius, H. & Jaenisch, R. (1984) *Proc. Natl. Acad. Sci. USA* **81**, 1504–1508.
10. Jahner, D. & Jaenisch, R. (1985) *Nature (London)* **315**, 594–597.
11. Breindl, M., Harbers, K. & Jaenisch, R. (1984) *Cell* **38**, 9–16.
12. Stacey, A., Mulligan, R. & Jaenisch, R. (1987) *J. Virol.* **61**, 2549–2554.
13. Schnieke, A., Dziadek, M., Bateman, J., Mascara, T., Harbers, K., Gelinas, R. & Jaenisch, R. (1987) *Proc. Natl. Acad. Sci. USA* **84**, 764–768.
14. Stacey, A., Bateman, J., Choi, T., Mascara, T., Cole, W. & Jaenisch, R. (1988) *Nature (London)* **332**, 131–136.
15. Bonadio, J., Saunders, T. L., Tsai, E., Goldstein, S. A., Morris-Wiman, J., Brinkley, L., Dolan, D. F., Altschuler, R. A., Hawkins, J. E., Bateman, J. F., Mascara, T. & Jaenisch, R. (1990) *Proc. Natl. Acad. Sci. USA* **87**, 7145–7149.
16. Deak, S. B., Van der Rest, M. & Prockop, D. J. (1985) *Collagen Relat. Res.* **5**, 305–313.
17. Sykes, B. C., Puddle, B., Francis, M. J. & Smith, R. (1976) *Biochem. Biophys. Res. Commun.* **72**, 1472–1480.
18. Frohman, M. A., Dush, M. K. & Martin, G. R. (1988) *Proc. Natl. Acad. Sci. USA* **85**, 8998–9002.
19. Scharf, S. J., Hern, G. T. & Erlich, H. A. (1986) *Science* **233**, 1076–1078.
20. Green, E. L. (1985) *Mouse News Lett.* **73**, 20–21.
21. Nicholls, A. C., Pope, F. M. & Schloon, H. (1979) *Lancet* **i**, 1193.
22. Nicholls, A. C., Osse, G., Schloon, H. G., Lenard, H. G., Deak, S. B., Myers, J. C., Prockop, D. J., Weigel, W. R., Fryer, P. & Pope, F. M. (1984) *J. Med. Genet.* **21**, 257–262.
23. Deak, S. B., Nicholls, A. C., Pope, F. M. & Prockop, D. J. (1983) *J. Biol. Chem.* **258**, 15192–15197.
24. Dickson, L. A., Pihlajaniemi, T., Deak, S. B., Pope, F. M., Nicholls, A. C., Prockop, D. J. & Myers, J. C. (1984) *Proc. Natl. Acad. Sci. USA* **81**, 4524–4528.
25. Pihlajaniemi, T., Dickson, L. A., Pope, F. M., Korhonen, V. R., Nicholls, A. C., Prockop, D. J. & Myers, J. C. (1984) *J. Biol. Chem.* **259**, 12941–12944.
26. Phillips, C. L., Lever, L. W., Pinnell, S. R., Quarles, L. D. & Wenstrup, R. J. (1991) *J. Invest. Dermatol.* **97**, 980–984.
27. Dutton, R. V. (1987) *Radiol. Clin. North Am.* **25**, 1211–1233.
28. Bullough, P. G., Davidson, D. D. & Lorenzo, J. C. (1981) *Clin. Orthop.* **159**, 42–57.
29. Young, I. D. & Harper, P. S. (1980) *Lancet* **i**, 432.
30. Thompson, E. M., Young, I. D., Hall, C. M. & Pembrey, M. E. (1987) *J. Med. Genet.* **24**, 390–405.
31. Green, M. C. (1989) in *Genetic Variants and Strains of the Laboratory Mouse*, eds. Lyon, M. F. & Searle, A. G. (Oxford Univ. Press, Oxford), 2nd Ed., pp. 12–403.
32. Massie, H. R., Aiello, V. R., Shumway, M. E. & Armstrong, T. (1990) *Exp. Gerontol.* **25**, 469–481.
33. Fisher, L. W., Denholm, L. J., Conn, K. M. & Termine, J. D. (1986) *Calcif. Tissue Int.* **38**, 16–20.
34. Fisher, L. W., Eanes, E. D., Denholm, L. J., Heywood, B. R. & Termine, J. D. (1987) *Calcif. Tissue Int.* **40**, 282–285.
35. Muriel, M. P., Bonaventure, J., Stanescu, R., Marteaux, P., Guènet, J. L. & Stanescu, V. (1991) *Bone* **12**, 241–249.
36. Chan, H., Hartung, S. & Breindl, M. (1991) *Mol. Cell. Biol.* **11**, 47–54.